GEAP-5093
JANUARY 1966

EURAEC
JOINT U.S.-EURATOM RESEARCH
AND DEVELOPMENT PROGRAM

PHYSICAL MODEL OF HEAT TRANSFER BEYOND THE CRITICAL HEAT FLUX

E.P. QUINN

U.S. ATOMIC ENERGY COMMISSION
CONTRACT AT(04-3)-189
PROJECT AGREEMENT 34

ATOMIC POWER EQUIPMENT DEPARTMENT
GENERAL ELECTRIC
SAN JOSE, CALIFORNIA

DISCLAIMER

EURAEC
GEAP-5093
Joint U. S. -Euratom
Research and
Development Program
January 1966

PHYSICAL MODEL OF HEAT TRANSFER BEYOND THE CRITICAL HEAT FLUX

E. P. Quinn

Prepared for the
U. S. Atomic Energy Commission
Contract AT(04-3)-189
Project Agreement 34
for the
Joint U. S. -Euratom
Research and Development Program

Printed in U.S.A. Available from the
Clearing House for Federal Scientific and Technical Information
National Bureau of Standards, U.S. Department of Commerce
Springfield, Virginia
Price: $2.00 per copy

ATOMIC POWER EQUIPMENT DEPARTMENT
GENERAL ELECTRIC
SAN JOSE, CALIFORNIA

2848-ENG-44
135-AG-2/66

LEGAL NOTICE

LN5

TABLE OF CONTENTS

LIST OF ILLUSTRATIONS

PREFACE

The United States and the European Atomic Energy Community (Euratom), on May 29, and June 18, 1958, signed an agreement which provides a basis for cooperation in programs for the advancement of the peaceful applications of atomic energy. This agreement, in part, provides for the establishment of a Joint U. S. -Euratom research and development program which is aimed at reactors to be constructed in Europe under the Joint Program.

The work described in this report represents the Joint U. S. -Euratom effort which is in keeping with the spirit of cooperation in contributing to the common good by the sharing of scientific and technical information and minimizing the duplication of effort by the limited pool of technical talent available in western Europe and the United States.

SECTION I

SUMMARY

A physical model of fully-developed film boiling, space-dependent film boiling, and transition boiling for high-pressure forced water flow is analyzed and compared to experimental measurements. An analytical expression is given for the heat transfer from the wall to superheated steam phase in film boiling. Empirical coefficients are shown for the heat transfer between the steam phase and entrained droplets. A relation is given for estimating over-all heat transfer coefficients for fully-developed film boiling. Spatially-dependent film boiling is examined and found to be a result of boundary layer and bulk steam phase superheat development.

SECTION II

INTRODUCTION

Extensive experimental measurements have been obtained of heat transfer behavior beyond the critical heat flux (CHF). These tests were run with forced flow at high pressure and intermediate steam qualities by Quinn[1] and Kunsemiller.[2] Beyond the CHF, wall temperature fluctuations are found to occur over a very narrow range of conditions. This region is referred to as the transition boiling region. As the heat input to the test assembly is further increased, stable film boiling takes place at high wall temperature levels. A representation of typical wall temperature behavior is given in Figure 2-1. The corresponding variation in heat transfer coefficient is also shown in Figure 2-1. Heat transfer coefficient data display a decreasing trend in the film boiling region labeled Region 2. This is attributed to a dependence on upstream dry-wall length involving thermal boundary layer development and bulk superheating of the steam phase, and is treated in detail in Reference 1. As the power input is further increased, Region 1 is entered where the coefficients are no longer directly dependent on the space variable but depend only on quality and steam phase superheat. Here the coefficients are found to rise gradually as vapor velocity increases with steam quality.

Concurrent measurement of wall temperatures at various positions along the heated wall and high-speed photography of heated surface fluid behavior during transition boiling[3] have led to the conclusion that in the flow regime studied, transition temperature fluctuations are caused by temporal undulations of the liquid film terminus on the wall. The effects of the oscillating movement of the liquid film terminus on heat transfer behavior are shown in Figure 2-2 * for the two extreme positions. The lowermost position is seen in the figure to be the location of the CHF condition. The uppermost position is near the location of the onset of stable film boiling, because the wall does not rewet beyond this position. However, significant variations in the heat transfer coefficient occur for a short distance beyond the uppermost film terminus position, making the transition boiling length slightly longer than the terminus travel.

The movement of the liquid film terminus is ordinarily very slow and travels over a short distance; namely, about 10 to 20 seconds per cycle and less than three hydraulic diameters for the single rod tests reported in Reference 1. Ordinary irregularities of two-phase flow and slight unsteadiness of loop conditions, such as small oscillations of absolute pressure, appear to be the cause of terminus movement. The spatial dependence of wall temperature and heat transfer coefficient beyond the transition boiling location are also shown in Figure 2-2.

*The heat flux is uniform and constant in the figure.

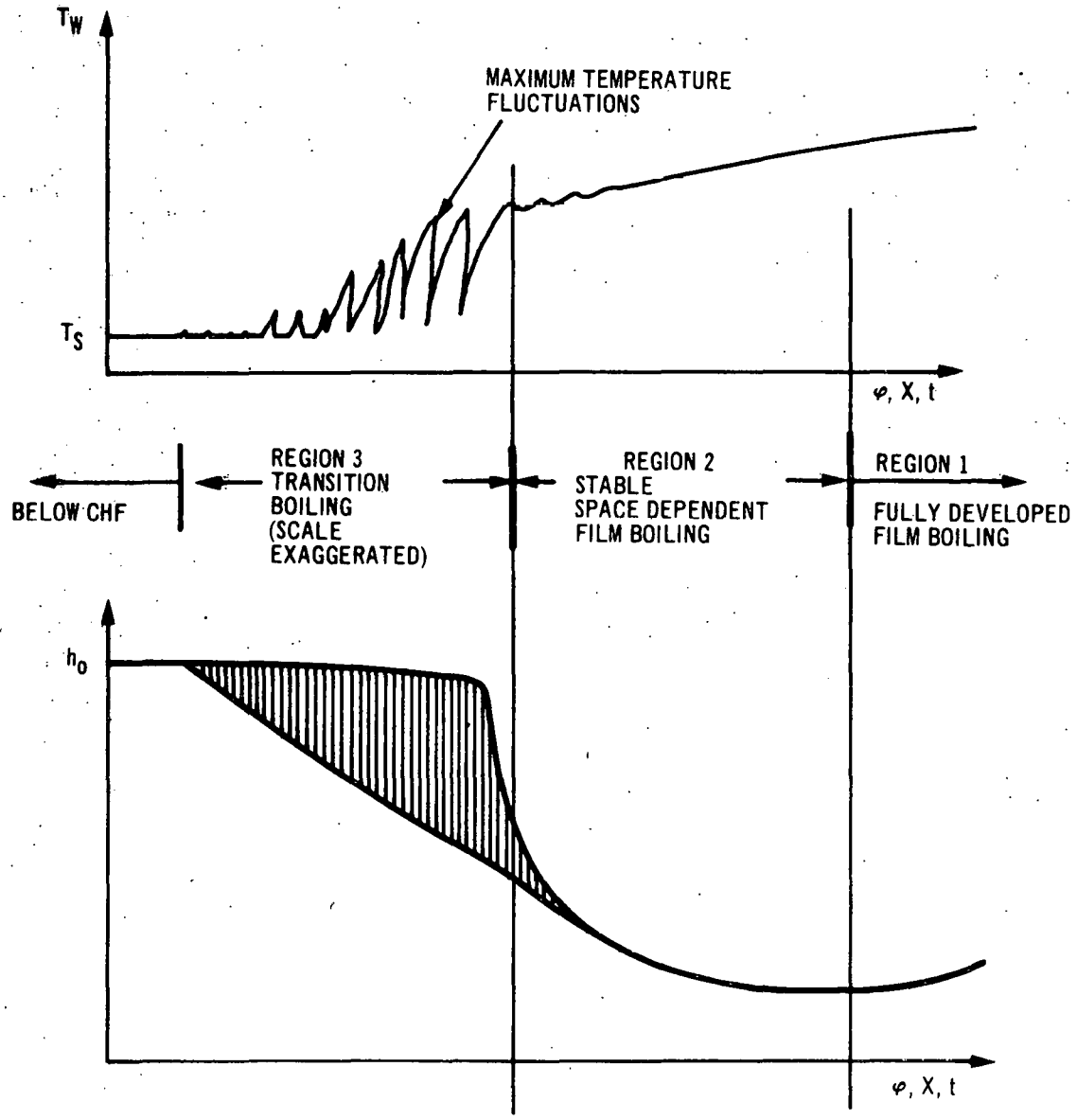

Figure 2-1. Typical Experimental Measurements at One Position with Increasing Power Input

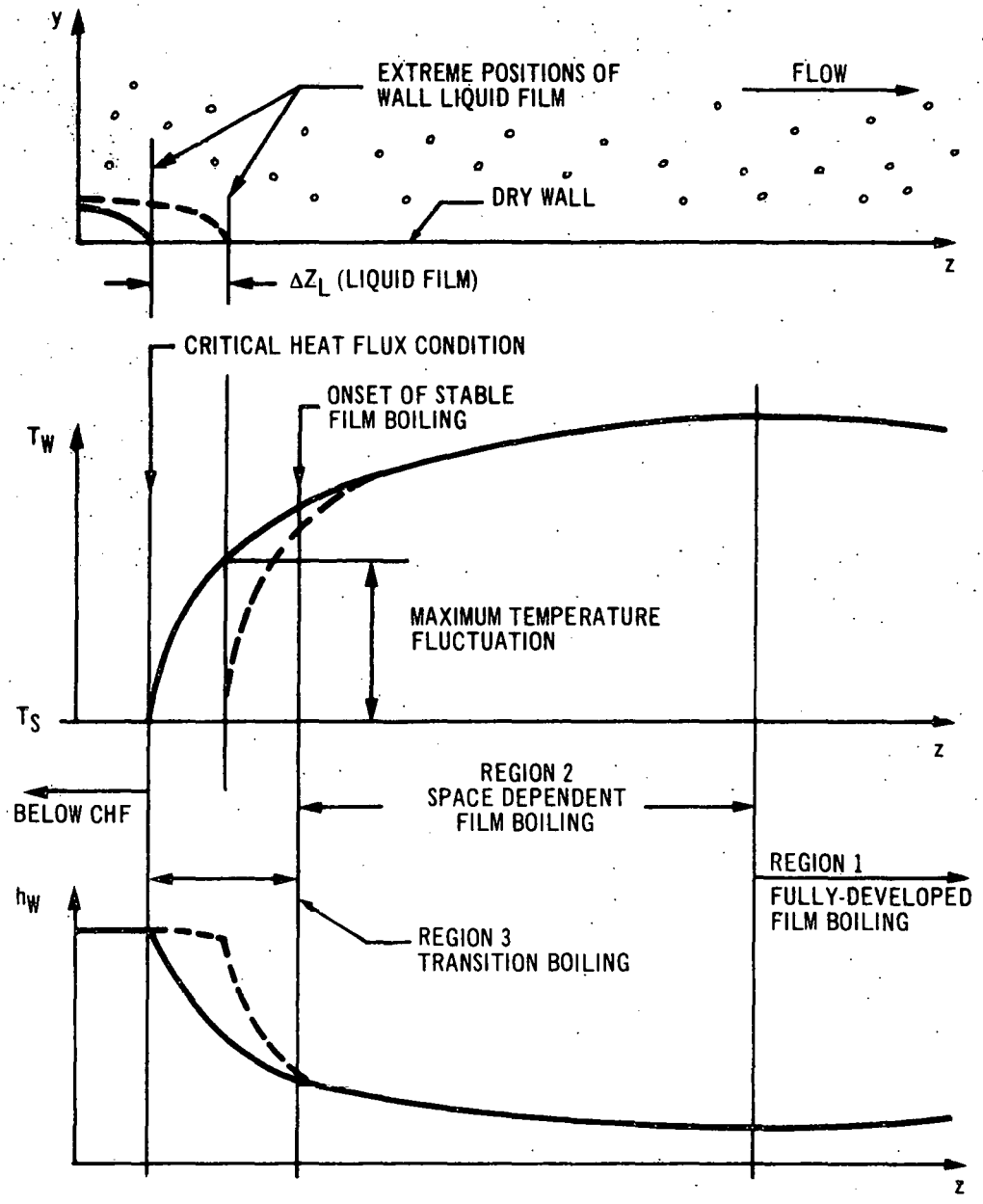

Figure 2-2. Heat Transfer Dependence on Space

It is interesting to note that the coefficient spatial effects cause the magnitude of the maximum temperature fluctuation to depend on the extent of liquid film travel. It should be kept in mind that excessive two-phase flow disturbances have been found to produce transition boiling over a very wide range of conditions, with the liquid terminus traveling over a very large distance [see Gaudiosi[4]].

It is well, at this point, to summarize the present picture we have of behavior beyond the critical heat flux. This is shown in outline form in Table 2-1. It is noted in the table that transition boiling behavior depends, in part, on space-dependent film boiling and that, in turn, depends in part on fully-developed film boiling. It appears that, in examining these three heat transfer regions, one must begin with fully-developed film boiling and work backwards to the critical heat flux.

TABLE 2-1

HEAT TRANSFER BEHAVIOR WITH GEOMETRY, MASS FLOW, AND HEAT FLUX CONSTANT

Region	Term	Characteristic	Governing Variables
1	Fully-Developed Film Boiling	Heat transfer coefficient	Steam quality Steam phase superheat
		a. Steam phase superheat	Water phase distribution
2	Space-Dependent Film Boiling	Heat transfer coefficient	Boundary layer and superheat development Region 1 coefficient
		a. Thermal boundary layer development	Dry-wall length
		b. Bulk steam phase superheat	Dry-wall length
3	Transition Boiling	Magnitude of maximum temperature fluctuations	Liquid film travel Region 2 coefficient
		a. Liquid film travel	Unsteady loop conditions Flow disturbance level
		b. Period of temperature fluctuations	Period of unsteadiness or flow disturbances
		Range of operating conditions for transition boiling	Degree of unsteadiness Flow disturbance level

SECTION III

FULLY-DEVELOPED FILM BOILING

Other measurements of film boiling coefficients for water near a 1000 psia have been taken by Sorlie,[5] Polomik, et al.,[6] Bennet, et al.,[7] Bennet and Kearsey,[8] and Hench.[9] It is necessary to examine the data published in the literature carefully, because most of the coefficients are not fully developed. Table 3-1 lists fully-developed heat transfer coefficients from these sources. The test geometries vary widely. Most of the data were taken on internally heated annuli, except for Hench (2 rod-facing unheated wall) and Kunsemiller (3 rod-facing unheated wall). Data taken by Bennet[8] for flow inside a heated tube are also listed for comparison.

It is of interest to compare the measured values in Table 3-1 with what can be computed from a single-phase heat transfer relation modified to account for the effect of the water present. The Sieder-Tate equation was chosen for this purpose:

$$h_W = 0.023 \left(\frac{\mu_B}{\mu_W}\right)^{0.14} \frac{k_B}{D_s} Pr_B^{1/3} \left(\frac{G_S D_S}{\mu_B}\right)^{0.8} . \qquad (1)$$

The Colburn equation should not be used for saturated or near-saturated steam because it depends on the ratio of bulk to film specific heats. The specific heat for steam exhibits strong temperature dependence in this region.

The properties of Equation (1) are clearly steam properties, since the wall is dry, except for possible impingement of liquid droplets. Parker and Grosh[10] discuss droplet impingement, and indicate that at a certain low value of wall-to-saturation temperature difference, the droplets reach a spheroidal state and rebound from the wall without appreciably cooling it. For the annular case, the mass velocity and diameter are those for the steam phase:

$$G_S = G_T \frac{X}{\alpha} , \quad D_S = \alpha D_H . \qquad (2)$$

All that is then needed to apply Equation (1) to two-phase flow is a relation for the void fraction. Any number of relations could be chosen for this purpose. Polomik's[11] equation is used here, because it agrees well with measurements above 20 percent quality and leaves the density ratio explicit:

$$\frac{1}{\alpha} = 1 + \frac{1-X}{X} \left(\frac{\rho_B}{\rho_f}\right)^{2/3} . \qquad (3)$$

TABLE 3-1

MEASURED FULLY-DEVELOPED HEAT TRANSFER COEFFICIENTS

Source	Geometry	D_H^* (in.)	P (psia)	G (10^6 lb/h-ft^2)	X_E	ϕ (10^6 Btu/h-ft^2)	T_W-T_S (°F)	h_o (Btu/h-ft^2-°F)
Quinn	Annular	0.375	1000	0.500	0.55	0.226	560	410
Sorlie	Annular	0.438	1000	0.515	0.435	0.194	975	195
	Annular	0.438	1000	0.777	0.361	0.236	991	238
	Annular	0.438	1000	1.048	0.306	0.267	937	285
Polomik	Annular	0.240	1100	1.12	0.523	0.306	369	830
	Annular	0.240	1100	1.52	0.452	0.340	328	1040
Bennet	Annular	0.250	1019	0.57	0.959	0.059	90	655
Hench	Two-Rod	0.234	1000	1.40	0.70+	0.600	766	790
Kunsemiller	Three-Rod	0.400	1400	1.00	0.345	0.275	466	590
	Three-Rod	0.326	1000	1.00	0.383	0.333	564	590
Bennet	Tube	0.497	1010	0.876	0.724	0.400	558	717
	Tube	0.497	1005	0.865	0.890	0.233	330	704
	Tube	0.497	995	0.845	0.931	0.332	502	661
	Tube	0.497	1007	0.895	0.974	0.217	292	743

*Local, based on twice rod to unheated wall spacing.

The combination yields a modified Sieder-Tate equation tentatively applicable for two-phase flow in an annulus:

$$h_W = 0.023 \left(\frac{\mu_B}{\mu_W}\right)^{0.14} \frac{k_B}{D_H} Pr_B^{1/3} \left(\frac{G_T D_H X}{\mu_B}\right)^{0.8} \left[1 + \frac{1-X}{X}\left(\frac{\rho_B}{\rho_f}\right)^{2/3}\right] . \quad (4)$$

The corresponding equation for flow inside tubes is:

$$h_W = 0.023 \left(\frac{\mu_B}{\mu_W}\right)^{0.14} \frac{k_B}{D_H} Pr_B^{1/3} \left(\frac{G_T D_H X}{\mu_B}\right)^{0.8} \left[1 + \frac{1-X}{X}\left(\frac{\rho_B}{\rho_f}\right)\right]^{0.8} . \quad (5)$$

There is no unheated, wetted surface in the tube case, so homogeneous flow over the whole tube diameter is a good physical basis for Equation (5). Equations (4) and (5) are plotted for 1000 psia and saturated bulk temperature in Figure 3-1. Steam properties were taken from Sutherland and Miller.[12] Neglecting droplet impingement, the values from Figure 3-1 are upper-bound values and are so listed in Table 3-2 for comparison with the measurements.

It is noted in Table 3-2 that the upper-bound values exceed the measurements by 20 to 50 percent for most cases. This can be stated by this inequality:

$$h_{UB}\ (T_S,\ X_E)\left[T_W - T_S\right] < h_o\ (\text{meas.})\left[T_W - T_S\right] . \quad (6)$$

It is recognized that the film boiling process must involve some bulk superheating of the vapor phase. This is a consequence of transferring wall heat to evaporate the saturated liquid phase via the steam phase. The effect of property variations with bulk temperature on the Sieder-Tate equation is shown in Figure 3-2. It is found that small amounts of bulk steam phase superheat can reduce the heat transfer coefficient considerably. Further, if bulk superheat is present, the actual quality is lower than the thermal equilibrium (measured) value. A lower actual quality serves to reduce further the coefficient one would compute. Finally, Equations (4) and (5) give only the heated wall coefficient, while the measured coefficient is necessarily lower because it involves a steam-to-liquid coefficient.

It is instructive to inquire as to how much superheat probably existed for the tests listed in Table 3-2. Equations (7) and (8) determine the value of T_B:

$$h_W\ (T_B,\ X_A)\left[T_W - T_B\right] = h_o\ (\text{meas.})\left[T_W - T_S\right] , \quad (7)$$

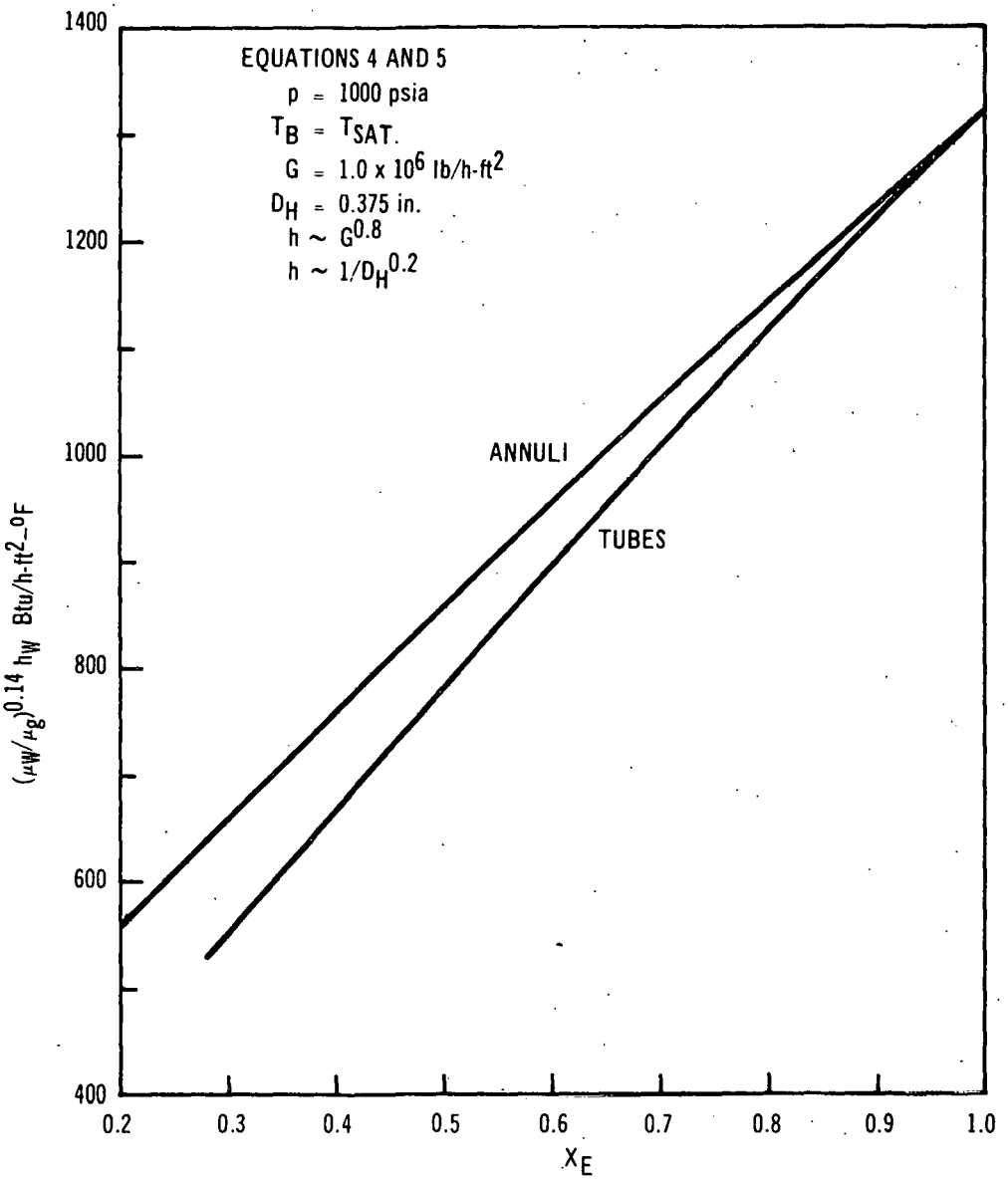

Figure 3-1. Sieder-Tate Equation for Two-Phase Flow for Saturated Bulk Steam Conditions

TABLE 3-2

COMPARISON OF MEASURED AND COMPUTED HEAT TRANSFER DATA

	Measured				Computed					
Source	ϕ (10^6 Btu/h-ft^2)	X_E	T_W-T_S (°F)	h_o (Btu/h-ft^2-°F)	h_{UB} ($T_B = T_S$) (Btu/h-ft^2-°F)	h_W (Btu/h-ft^2-°F)	T_B-T_S (°F)	X_A	H (Btu/h-ft^2-°F)	$\frac{T_B-T_S}{T_W-T_S}$ (%)
Quinn	0.226	0.55	560	410	491	436	35	0.52	6110	6.2
Sorlie	0.190	0.435	975	195	412	274	284	0.33	504	29
	0.236	0.361	991	238	518	342	300	0.27	583	30
	0.267	0.306	937	285	608	406	202	0.23	713	30
Polomik	0.306	0.523	369	830	1017	909	32	0.49	9030	8.7
	0.340	0.452	328	1040	1190	1101	18	0.44	18300	5.5
Bennet	0.059	0.959	90	655	885	823	19	0.93	3000	21
Hench	0.600	0.70$^+$	766	790	1140	890	85	0.62	6270	11
Kunsemiller	0.275	0.345	466	590	813	662	52	0.31	4750	11
	0.333	0.383	564	590	760	645	49	0.35	6300	8.7
Bennet	0.400	0.724	558	717	822	751	25	0.69	15400	4.5
	0.233	0.890	330	704	995	832	52	0.82	4140	16
	0.332	0.931	502	661	984	770	75	0.84	3980	15
	0.217	0.974	292	743	1083	900	52	0.90	3840	18

$$X_A = X_E \left[1 + \frac{h_B - h_g}{h_{fg}} \right]^{-1} \quad (8)$$

To aid in solving Equation (7), the ratio of h_W (T_B, X_A) to h_{UB} (T_S, X_E) is plotted in Figure 3-3 as a function of bulk superheat. It can be used as a multiplier for values taken from Figure 3-1. The results of applying Equation (7) to the data are tabulated in Table 3-2 as the wall coefficient, bulk steam phase superheat, and the actual steam quality. Except for Sorlie's data, the degree of superheat is found to be a very small percentage of the wall-saturation temperature difference. This indicates, with one exception, very good heat transfer between the steam and liquid phases. This heat transfer coefficient, H, based on heated surface area is listed in Table 3-2. In computing H, the heat flux is that for evaporation only; the balance to superheat the evaporated saturated vapor is assumed to be transferred by mixing. The heat transfer to the wetted wall can be easily estimated (see Reference 1). The wetted wall coefficients are in the range of 500 to 1000 Btu/h-ft^2 -°F for these data. The much larger values of H must mean that most of the heat is absorbed by droplets in the main stream.

Values of H computed from tests involving a wide range of conditions and geometries are plotted in Figure 3-4. Further support is given to the postulate that the droplets dominate the steam-liquid heat transfer by the fact that Bennet's tube data, where there is no wetted wall, fall in with the annular data in Figure 3-4. Also, Kunsemiller[2] finds similar coefficients between two heated rods and a rod and unheated wall on his three-rod assembly. Except for Sorlie's data, H ranges from 4,000 to 18,000 Btu/h-ft^2 -°F in Figure 3-4. A good estimate of fully-developed film boiling coefficients may be obtained by using the modified Sieder-Tate equation and a mean of these values of H. H values range plus or minus 64 percent about the mean for this wide condition range. The over-all coefficient may be computed from Equation (9):

$$\frac{1}{h_o} = \frac{1}{h_W(T_B, X_A)} + \frac{1}{H\left[1 + \frac{h_B - h_g}{h_{fg}}\right]} \quad (9)$$

The calculation of h_o is insensitive to the exact value of H, since $h_W \ll H$. Alternately, the volume heat absorption coefficient of Figure 3-5, which takes account of differences in test geometry, may be used.

It remains to discuss the possible causes of Sorlie's coefficients, h_o and H, being so low and his superheat so high: 30 percent of (T_W-T_S). First, the heat transfer coefficient from the superheated steam to the liquid wetting the unheated wall can be estimated by following the technique of Reference 1. It is assumed that all the water lies on the unheated wall, the liquid

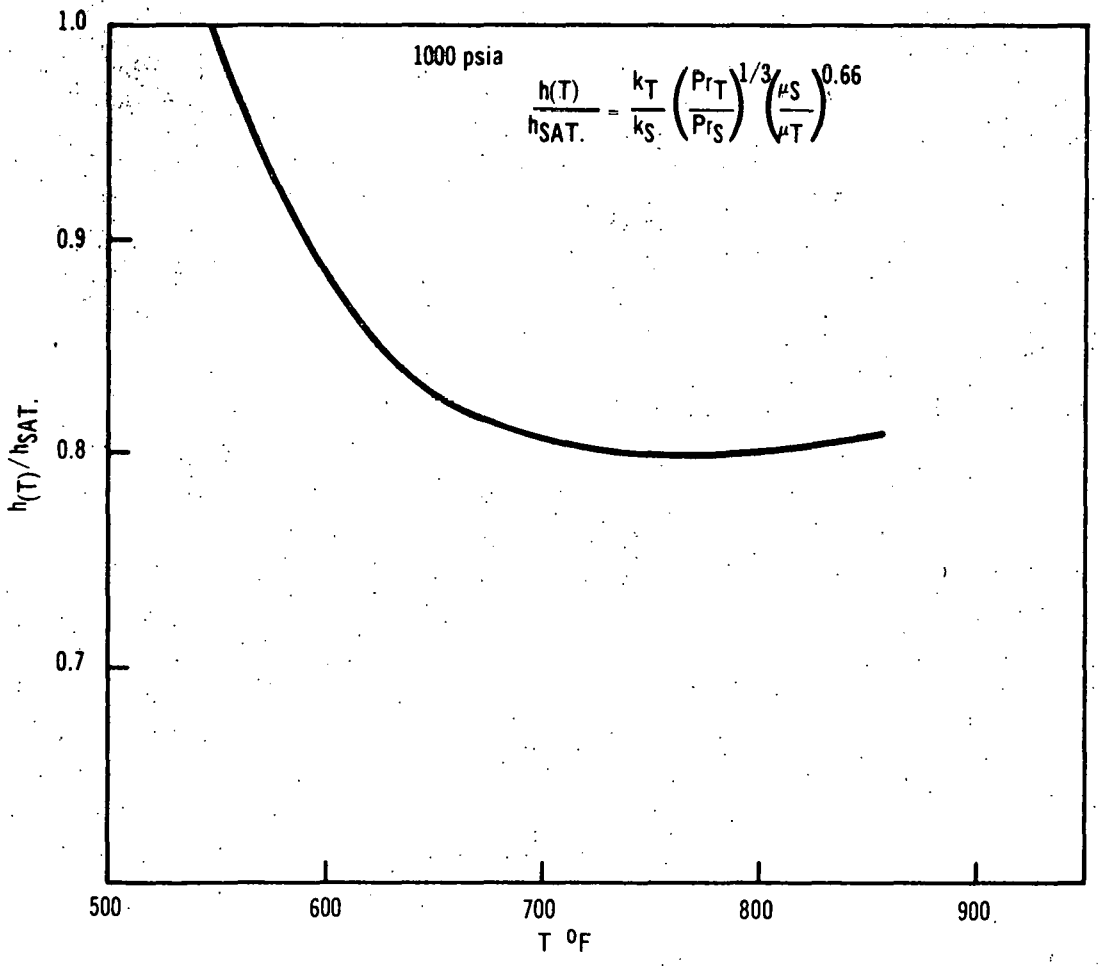

Figure 3-2. Effect of Properties on Wall Heat Transfer Coefficient for Sieder-Tate Equation

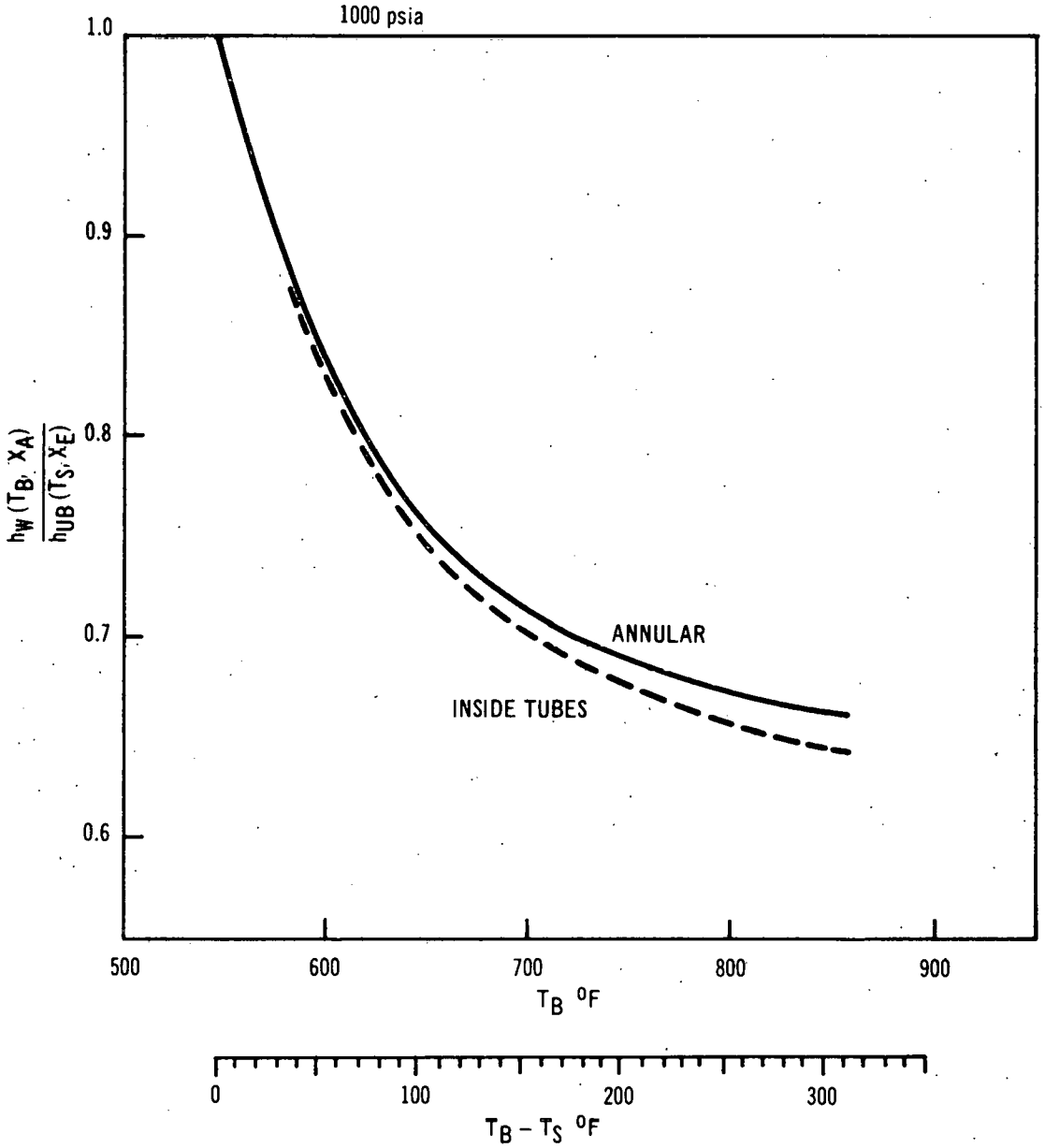

Figure 3-3. Effect of Superheat on Wall Coefficients

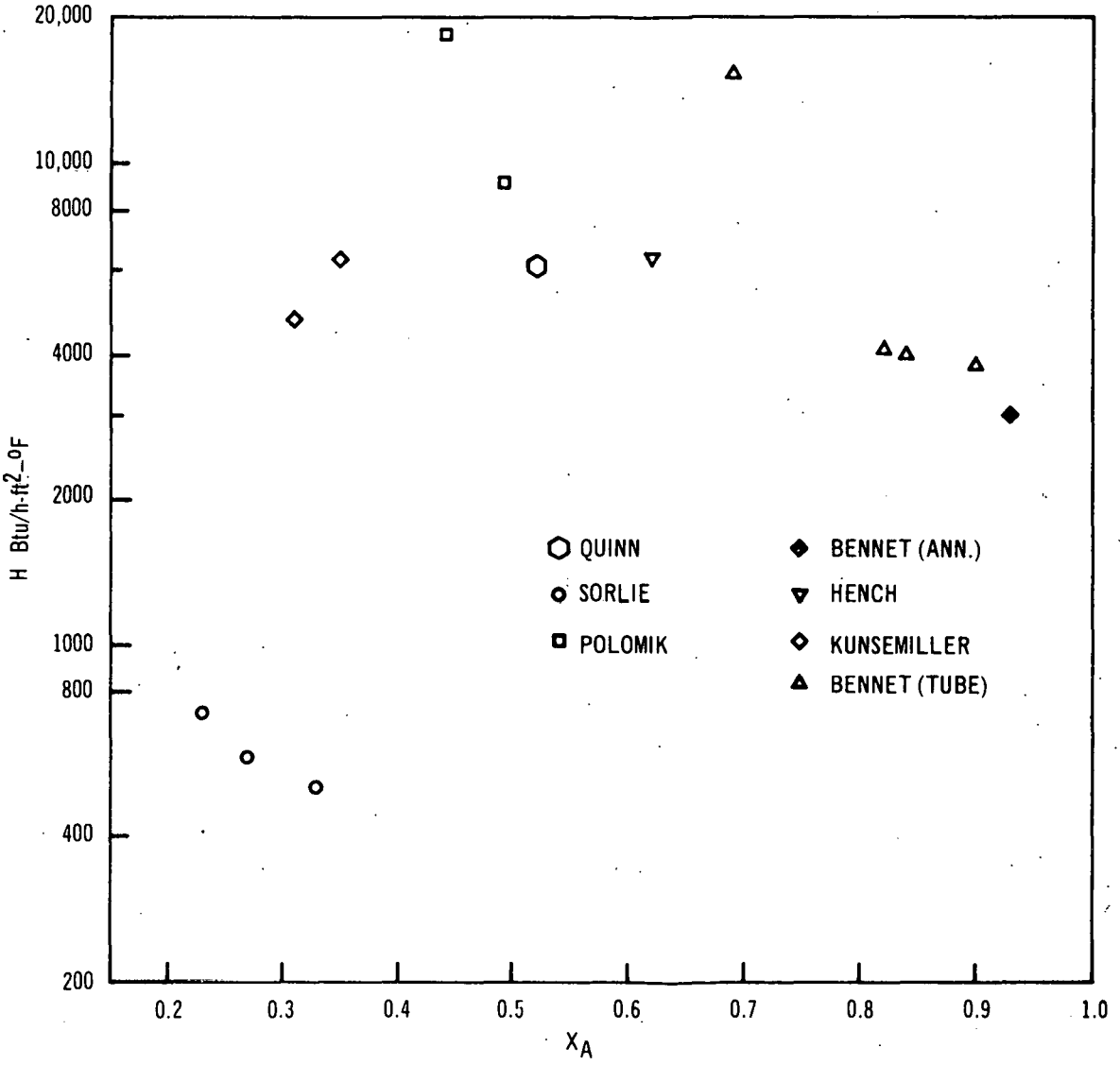

Figure 3-4. Heat Absorption Coefficient Based on the Heated Surface Area

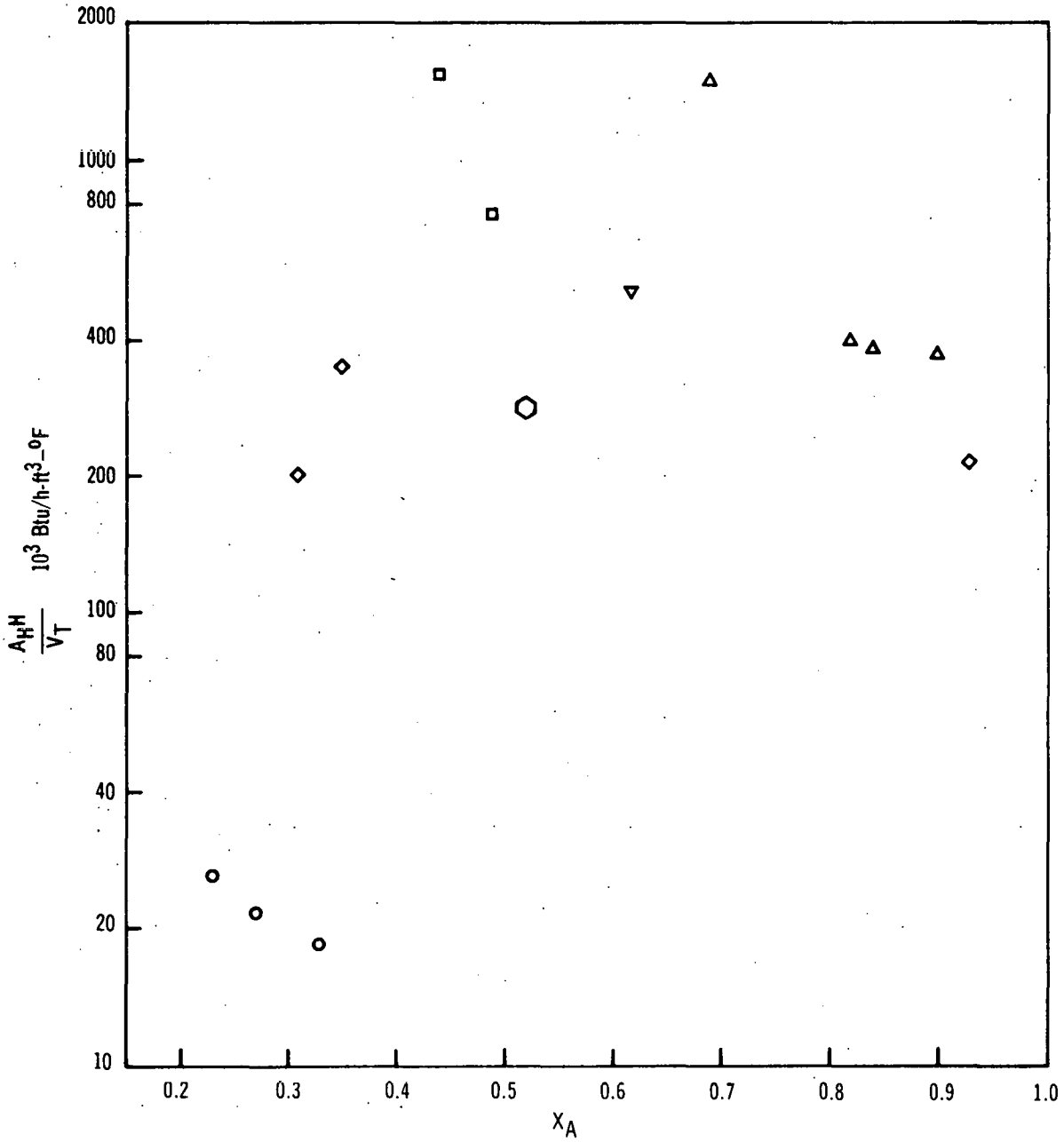

Figure 3-5. Volume Heat Absorption Rate

surface is smooth, and the slip can be calculated from Polomik's void fraction. The coefficient for the steam-to-liquid covered wall is the following:

$$h_L = 0.023\left(\frac{\mu_B}{\mu_g}\right)^{0.14}\frac{k_B}{D_H}\,Pr_B^{1/3}\left[\frac{G\,D_H X_A}{\mu_B}\right]^{0.8}\left[1-\left(\frac{\rho_B}{\rho_f}\right)^{1/3}\right]^{0.8}\left[1+\frac{1-X_A}{X_A}\left(\frac{\rho_B}{\rho_f}\right)^{2/3}\right]$$

$$H_L = \left[1+\alpha\frac{D_H}{d}\right]h_L \,. \qquad (10)$$

It is seen in the following table that the H values for Sorlie's data can be nearly accounted for by heat transfer to the liquid-covered wall computed by Equation (10).

H (total) (Btu/h-ft^2-°F)	H_L (Btu/h-ft^2-°F)	H_D(to droplets) (Btu/h-ft^2-°F)
504	412	92
583	502	81
713	575	138

The conclusion for Sorlie's tests is that very little water was carried along with the steam in droplet form. This condition may occur for a large upstream dry heated surface if very little water is entrained from the unheated wall.

This exploration gives additional insight into the factors and the order of magnitude of variables affecting the film boiling process. A means of estimating heat transfer coefficients has also been developed. More work is of course needed before fully-developed film boiling coefficients can be computed accurately. Certainly more experimental data are needed, preferably together with measurements of bulk steam phase superheat. The role of droplet impingement on the heated surface should be evaluated. A major effort should be directed toward predicting the value of H as it determines the steam superheat level. The value of H depends on three things:

a. Droplet concentration,
b. Droplet size, and
c. Droplet agitation.

They are analyzed by Laverty and Rohsenow[13] for nitrogen.

The droplet concentration is unknown and difficult to estimate where an unheated surface is present. It depends on the history of the two-phase flow from where boiling begins, and the behavior near the critical heat flux condition. Test geometry and unusual test entrance conditions such as a two-phase inlet condition will change the concentration and size of droplets. Polomik, Hench, and Bennet used a two-phase inlet condition. A proposed extension of the current program should provide the basis for accurate prediction of fully-developed film boiling. It will include measurement of steam phase superheat.

SECTION IV

SPACE-DEPENDENT FILM BOILING

It is of interest to explore the spatial variation of the film boiling coefficient. The type of variation observed has been shown in Figure 2-2. Quinn[1] and Kunsemiller[2] show plots of experimental measurements with this trend. It may not be too important to establish the exact nature of coefficient space variation. Rather, the first step should be to determine the magnitude of the (dry-wall) distances required to attain fully-developed heat transfer and check the postulated causes of the coefficient variation. The postulated causes, as have been mentioned, are the following:

a. Thermal boundary layer development, and
b. Developing bulk steam phase superheat.

The physical picture we have for the development of film boiling is a dry, uniform heat flux surface which begins at the terminus of the wetting liquid film (see Figure 2-2). The wall at the terminus position is essentially at the saturation temperature. The wall temperature increases with downstream distance until a thermal boundary layer is developed and the bulk steam phase is superheated to establish heat transfer equilibrium. The terminal position of the liquid film on the heated surface may move slowly enough (over the short transition boiling length) for a steady-state temperature distribution to be assumed to exist in the heater wall and fluid. Simplified models for boundary layer and superheat development will be derived next.

4.1 THERMAL BOUNDARY LAYER

Boundary layer development analyses in the literature for single-phase flow present only graphical results, not suitable for comparing with experimental data. An approximate relation will be derived here.

The steam velocity distribution is already fully developed where the dry wall begins. The Reynolds' analogy for Prandtl number of unity will be applied to the thermal layer growth. Prandtl number for high-pressure steam is 0.9 for the large superheats near the wall. To simplify the analogy, the velocity distribution will be taken as uniform [$U(y,z)$ = constant]. The Reynolds number of interest for Table 3-1 is 10^5 to 2×10^5. The treatment is for annuli with a radius ratio near one so that the maximum velocity location is near the mean radius.

The analogy for fully-developed film boiling is the following, where R is half the annulus gap:

$$\frac{h_W(\infty)}{\rho U C_p} = \frac{f}{8} = \frac{0.023}{\left(\frac{4RU}{\nu}\right)^{0.2}} \quad (11)$$

The relation for dependence on space is similar:

$$\frac{h_W(z)}{\rho U C_p} = \frac{0.023}{\left[\frac{4\delta_T(z)U}{\nu}\right]^{0.2}} \quad (12)$$

The temperature - thermal layer thickness relation is clear from the equations:

$$\frac{T_W(z)-T_B(z)}{T_W(\infty)-T_B(\infty)} = \frac{\Delta T_W(z)}{\Delta T_W(\infty)} = \left[\frac{\delta_T(z)}{R}\right]^{0.2} \quad (13)$$

The radial variation of temperature is taken to follow the power law where n = 9 is required to be consistent with Equation (11):

$$\frac{\Delta T(y,z)}{\Delta T_W(z)} = 1 - \left(\frac{y}{\delta_T}\right)^{1/9} \quad (14)$$

The boundary layer buildup is governed by energy storage:

$$\frac{\phi}{\rho U C_p} = \frac{d}{dz}\int_0^{\delta_T(z)} \Delta T(y,z)\, dy = \frac{1}{10}\frac{d}{dz}\delta_T \Delta T_W \quad (15)$$

Combining Equations (13) and (11) with (15) gives the result:

$$\frac{h_W(z)}{h_W(\infty)} = \left[\frac{Re_\infty^{0.2}}{0.023 \times 4 \times 10}\frac{4R}{z_{B.L.}}\right]^{1/6} = \left[\frac{\left(\frac{G D_H X_A}{\mu_B}\right)^{0.2}}{0.92}\frac{D_H}{z_{B.L.}}\right]^{1/6} \quad (16)$$

The distance required to develop the thermal boundary layer is the following:

$$\left(\frac{z_{B.L.}}{D_H}\right)_\infty = 1.09\left(\frac{G D_H X_A}{\mu_B}\right)^{0.2} \quad (17)$$

The distance to build up the thermal boundary layer is then 10.9 hydraulic diameters for Re = 100, 000. This result agrees generally with the entrance length data of Hartnett[14] and the rigorous (and complex) analysis of Deissler.[15] The variation of wall coefficient with z is shown in Figure 4-1.

An uncertainty enters in relating measurements of coefficient spatial variation with the upstream dry-wall length. The coefficients are usually plotted versus heat flux (power input) beyond the critical heat flux, since the exact position of the wall liquid terminus is not continuously measured in the heat transfer tests. The dry surface area of a uniformly heated rod has been found in tests to be generally as shown in Figure 4-2. The spacers necessary to center the rod and avoid thermal bowing cause the surface just downstream of the spacers to remain wetted after the CHF location has moved upstream to lower quality positions. Care has been taken to make the spacers as small in cross section as possible for the three-rod tests of Kunsemiller.[2] The location of the lowermost dry surface can be established from the CHF on a local quality basis. The downward spread of the dry area within one span as the power input (heat flux, quality) is increased is much more gradual.

While liquid remains at one end of the instrumented span of the rod, a thermal boundary layer must develop in that span. For small, fully-developed superheat levels, the bulk steam will already be superheated by the upstream dry surfaces. In this case, the coefficient relation with space, Equation (16), can be compared with data, neglecting bulk superheat development when the ultimate superheat is small. The experimental coefficients of Reference 1 were plotted against heat flux. Also, the CHF and onset of steady film boiling were plotted against heat flux for four positions along the instrumented span. The latter plot yields a relation between time average upstream dry length and heat flux:

$$\frac{z}{D_H} = 133\,\frac{\phi-\phi_c}{\phi} \quad . \tag{18}$$

It is not strictly applicable to the geometry on which the heat transfer data were taken; however, the trend is of the right order of magnitude. By contrast, the local critical quality condition would predict Equation (19) for this particular geometry:

$$\frac{z}{D_H} = 894\,\frac{\phi-\phi_c}{\phi} \quad . \tag{19}$$

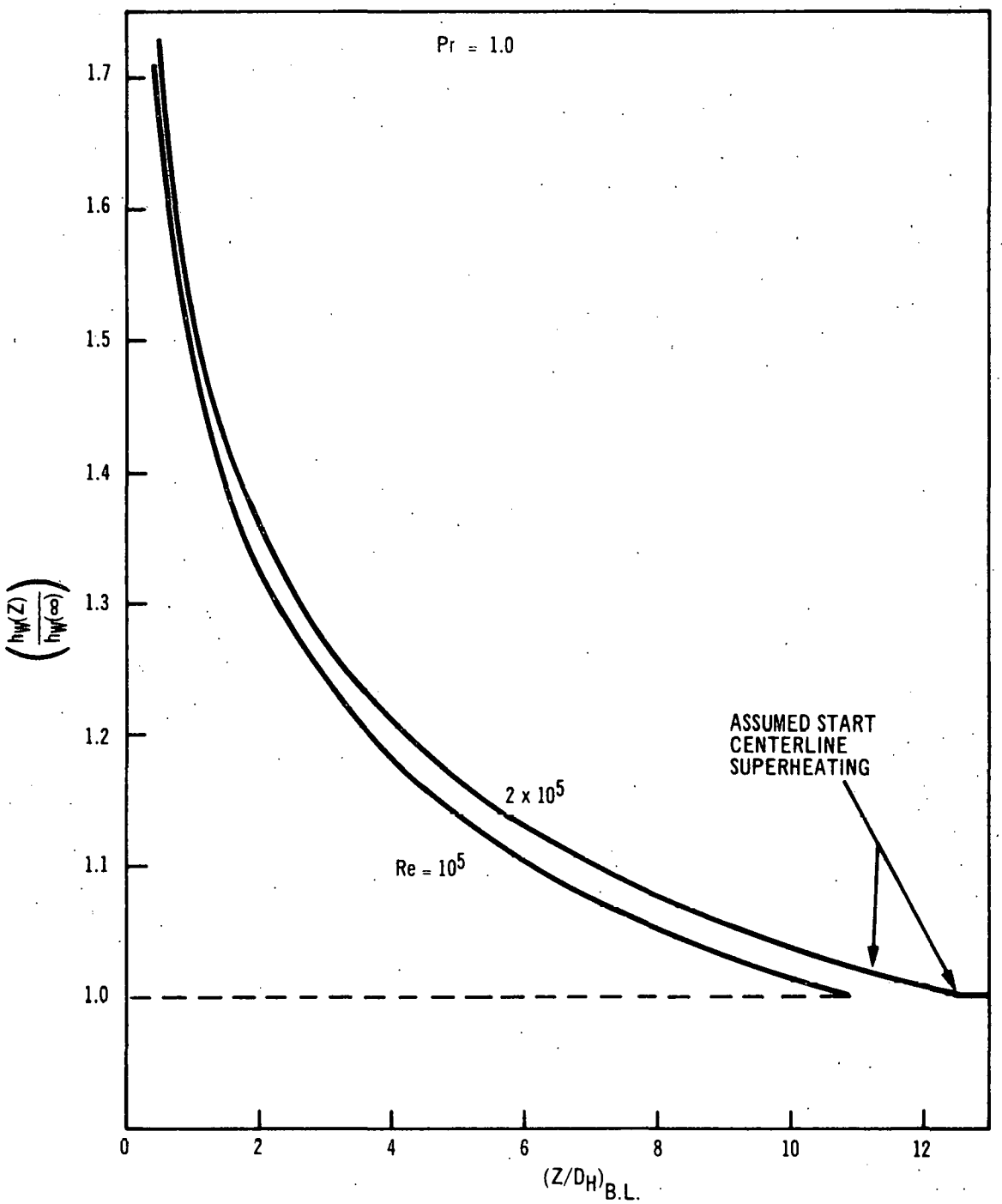

Figure 4-1. Plot of Equation 16

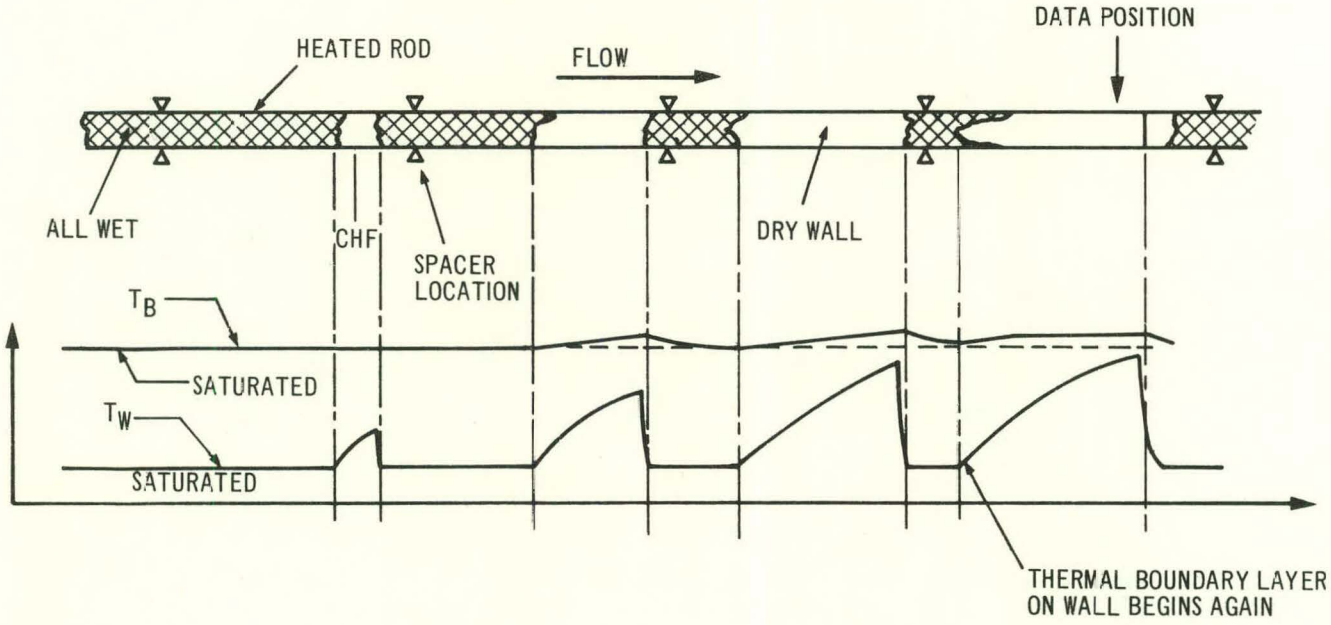

Figure 4-2. Typical Test Rod Temperature Distribution

Using Equation (18) to relate the experimental data to space yields the points on Figure 4-3. The agreement with the prediction is in part fortuitous. The expression $z_{W\infty}$ [Equation (17)] might not agree so well with the measurement if the exact coefficient in Equation (18) were known. However, since $z_{W\infty}$ does match, a comparison of the space variation may be made. The data follow nearly the same curve as the prediction, being high for small z values as expected since conduction in the wall was neglected.

The spatial variation given by Equation (16) is of course approximate, but it should be useful in estimating boundary layer development lengths and coefficient values. Rigorous single-phase relations from the literature may be used for more accuracy, and applied to this two-phase behavior as was done in the preceding example.

The order-of-magnitude agreement between experiment and prediction indicates that thermal boundary layer development dependent on space is indeed the cause of the measured declining film boiling coefficients.

4.2 BULK SUPERHEATING

Besides the dry-wall distance to develop the thermal boundary layer, additional length is required to superheat the main stream of the steam. The CHF occurs at a given quality, X_o, after which all the heat goes to superheat the steam phase and increase the quality beyond X_o. The heat balance on the bulk two-phase flow is:

$$\pi d \phi z = W C_p X(z) \Delta T_B(z) + W h_{fg} \left[X(z) - X_o\right] . \tag{20}$$

The heat transferred from the steam to the liquid is given by Equation (21) with H assumed constant:

$$\pi d H \Delta T_B(z) = W h_{fg} \frac{dX}{dz} . \tag{21}$$

Equations (20) and (21) are combined to eliminate X:

$$\left(\frac{C_p}{h_{fg}} z + \frac{W X_o C_p}{\pi d \phi}\right) \frac{d \Delta T_B}{dz} = \left(1 + \frac{C_p}{h_{fg}} \Delta T_B\right) \left[1 - \left(\frac{W C_p}{\pi d}\right)^2 \frac{1}{\phi H} \left(1 + \frac{C_p}{h_{fg}} \Delta T_B\right) \Delta T_B\right] . \tag{22}$$

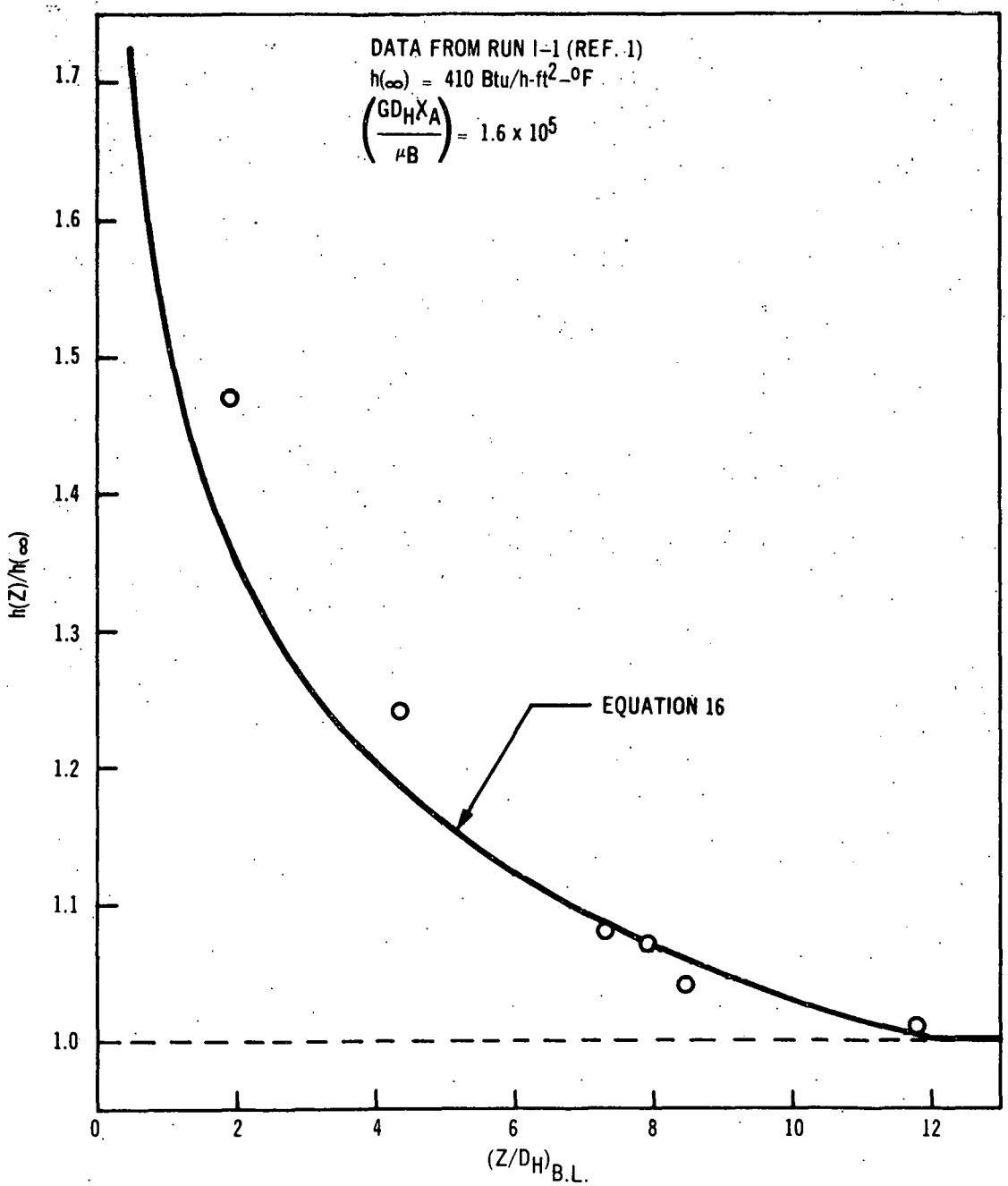

Figure 4-3. Comparison of Computed and Measured Coefficient Spatial Variation

Equation (22) is integrated to give the following result where L is the net boiling length, including the dry length:

$$\left(\frac{z}{L}\right)_{SUP.} = 1 - \frac{\left(1-S\right)^{\frac{k}{1+2k}} \left(1 + \frac{k}{1+k} S\right)^{\frac{1+k}{1+2k}}}{(1 + k S)} \tag{23}$$

$$S(z) = \frac{T_B(z)-T_S}{T_B(\infty)-T_S} \qquad k = \frac{C_p\left[T_B(\infty)-T_S\right]}{h_{fg}} = \frac{\sqrt{1 + \frac{4 C_p \phi}{h_{fg} H}} - 1}{2} .$$

The solution for the spatial dependence of bulk superheat is plotted in Figure 4-4.

4.3 COMBINED BOUNDARY LAYER AND SUPERHEAT DEPENDENCE

The over-all heat transfer coefficient is given by Equation (24):

$$\frac{1}{h_o(z)} = \frac{1}{h_W(z)} + \frac{T_B(z)-T_S}{\phi} . \tag{24}$$

Evaluating Equation (24) beyond the fully-developed position and forming a ratio gives the expression for space-dependent film boiling coefficients:

$$\frac{h_o(z)}{h_o(\infty)} = \frac{(T_W-T_S)_\infty}{(T_W-T_B)_\infty \frac{h_W(\infty)}{h_W(z_{B.L.})} + (T_B-T_S)_\infty S(z_{SUP.})} . \tag{25}$$

With no interruption in the dry-wall length, $z = z_{B.L.} + z_{SUP.}$, where the boundary layer is formed over $z_{B.L.}$ first (with s = 0) and then the superheat is attained over $z_{SUP.}$

Equation (25) may be used to compute coefficient spatial dependence, where $h_W(z)$ and S(z) are obtained from Equations (16) and (23) (or Figure 4-4).

The distance $(z_{SUP.})_{95\ percent}$ for $h_o(z)$ to reach 5 percent of $h_o(\infty)$, after the thermal layer has been developed, has been computed from Equations (23) and (25). It is plotted in Figure 4-5. The computed boundary layer and superheat distances are tabulated in Table 4-1 for the measurements from the sources previously examined for the fully-developed case. Only those that had a subcooled entrance with no change in flow cross section are considered.

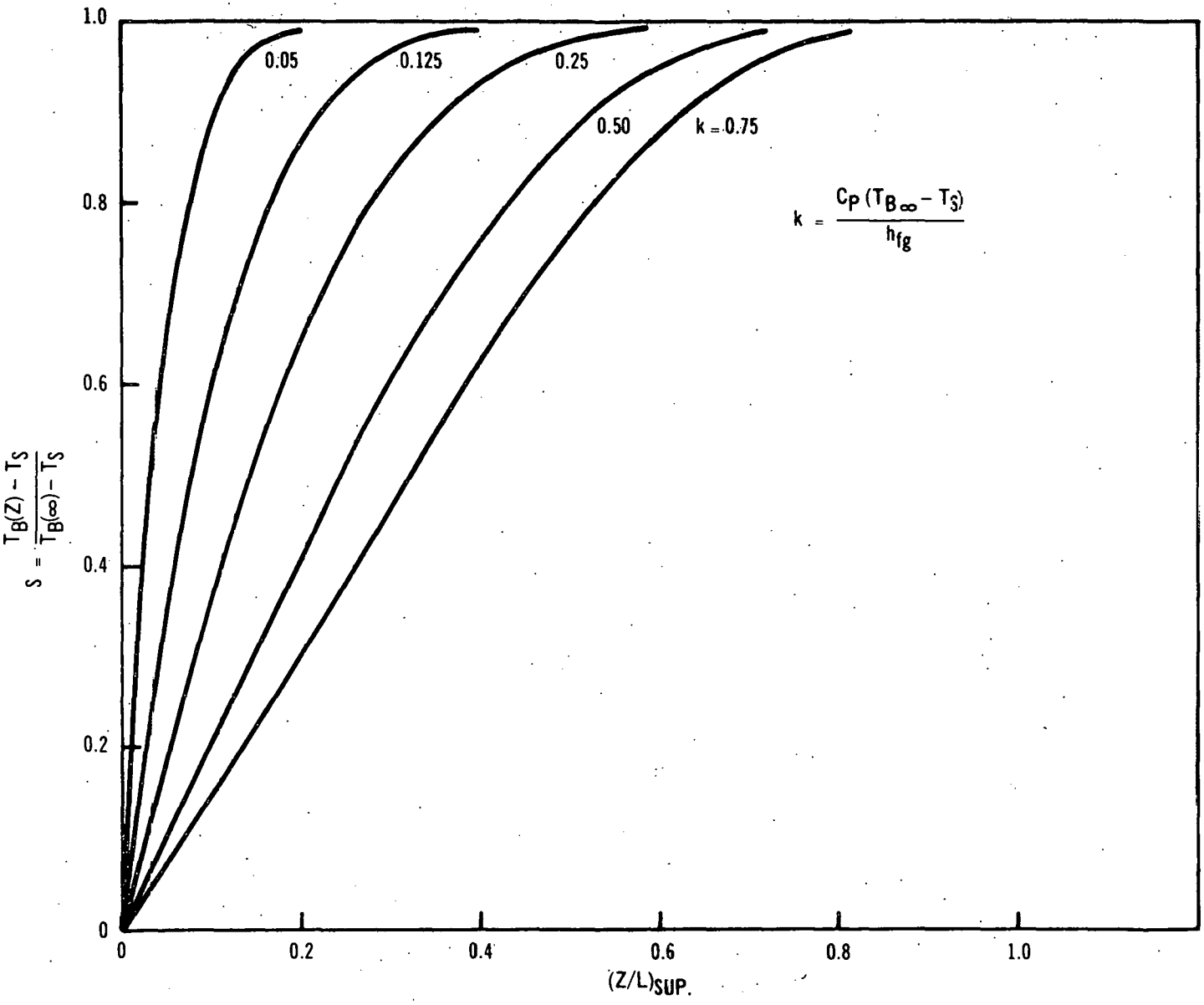

Figure 4-4. Bulk Steam Phase Superheat versus Dry Wall Length

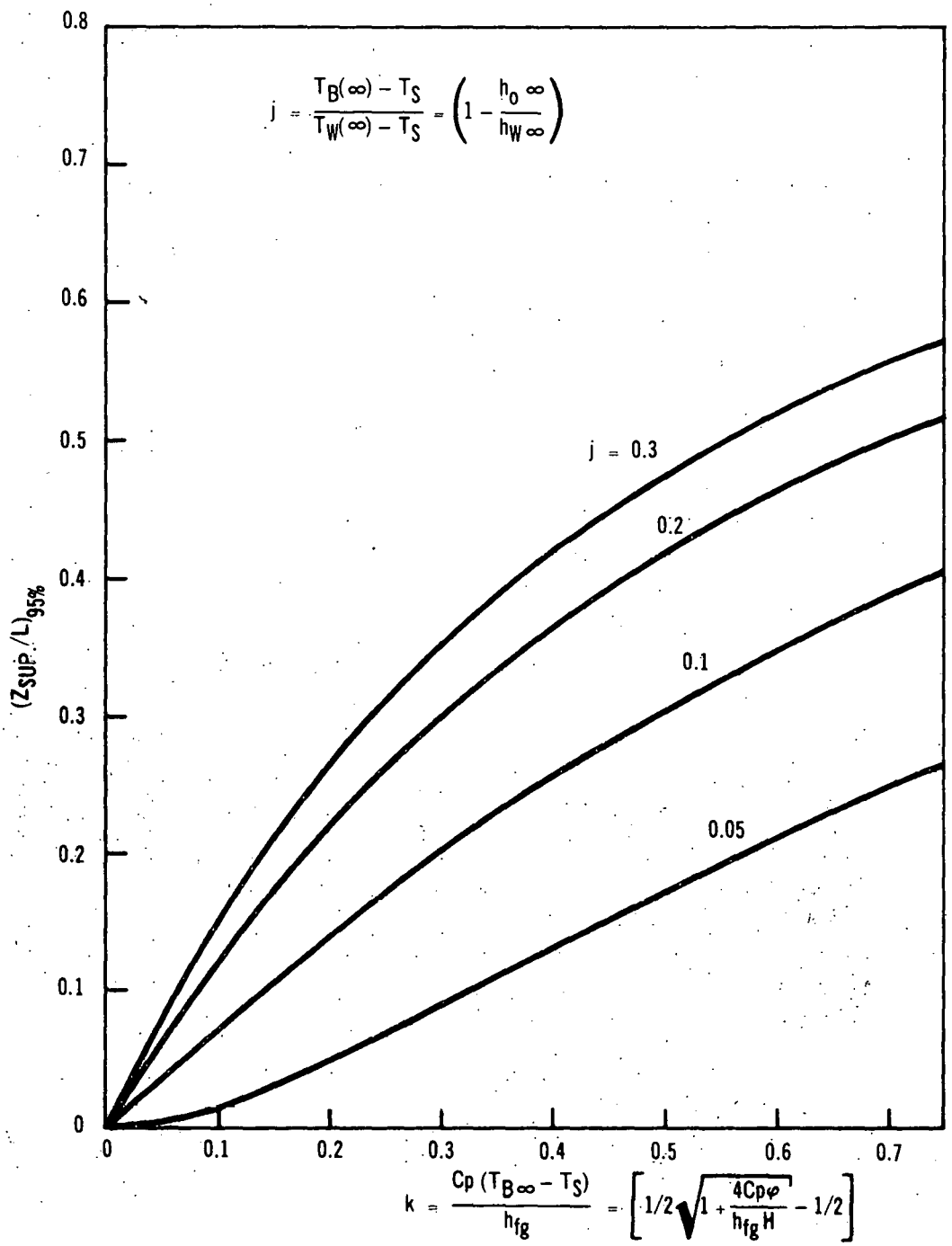

Figure 4-5. Bulk Superheat Length to Establish 95 percent Fully-Developed Film Boiling Coefficients

As may be seen in Table 4-1, the boundary layer distance is greater than the superheat distance for Quinn's data point. As was assumed before, the superheat should be fully developed before the instrumented span is reached and the measured coefficient variation dependent only on thermal layer buildup. Kunsemiller's superheat distance is a little larger than his boundary layer distance; his superheat was probably nearly developed before his last instrumented span as in Figure 4-2. His measured coefficients are also dominated by thermal layer growth.

Sorlie's data again shows different behavior. It is seen that his length to develop superheat is about 18 times as long as to develop the thermal layer. Sorlie's measurements are superheat dominated. Over one-third of his heated length must have been dry, to reach fully-developed film boiling. This, incidentally, is in agreement with his post-test examination of thermal markings on his heater rod. He found discoloration on the rod over the last 200 hydraulic diameters.

Generally, the declining trend of measured heat transfer coefficients before full development is attained has been shown to be related to dry-wall distance. This effect appears to be explained by thermal boundary layer development and storage of heat in the steam phase.

TABLE 4-1

DRY WALL LENGTHS TO DEVELOP FILM BOILING

Source	$\frac{L_{SPAN}}{D_H}$	$\frac{L_{TOT.}}{D_H}$	10^{-5} Re	$\frac{z_{B.L.}}{D_H}$	$\frac{C_p(T_{B\infty}-T_S)}{h_{fg}}$	$\frac{T_{B\infty}-T_S}{T_{W\infty}-T_S}$	$\left(\frac{z_{SUP.}}{L}\right)_{95\%}$
Quinn	24	683	1.60	12.0	0.058	0.062	0.010
Sorlie	41	562	0.97	10.8	0.331	0.29	0.370
	41	562	1.19	11.3	0.345	0.30	0.375
	41	562	1.37	11.6	0.328	0.30	0.370
Kunsemiller	22	445	1.95	12.4	0.115	0.11	0.085
	28	546	1.85	12.3	0.080	0.087	0.045

SECTION V

MAXIMUM TEMPERATURE FLUCTUATIONS DURING TRANSITION BOILING

The location and physical explanation of maximum temperature fluctuations has been illustrated in Figure 2-2. The largest fluctuation is assumed to occur at the location where the liquid terminus reaches its most downstream position. The largest temperature fluctuation occurs one-half cycle of terminus travel later when the upstream dry-wall length for this position is longest. The size of the largest temperature fluctuation depends on the maximum liquid film travel and the coefficient space dependence. If the terminus travel, Δz_L, is known, an instantaneous heat transfer coefficient or maximum temperature fluctuation may be computed from Equation (16). The coefficient in this case is a lower bound, since the computation assumes quasi-static behavior.

As an example, this can be done for the test run of Reference 1 for which fully-developed characteristics have been listed in Table 3-2. The maximum fluctuation was 129°F at a heat flux of 208,000 Btu/h-ft^2. The instantaneous over-all coefficient was then 1610 Btu/h-ft^2-°F. The superheat was small, so that this is nearly equal to the wall coefficient. From the plot of this test data in Figure 4-3, z/D_H for the onset of film boiling was about 1.9. As mentioned earlier and diagrammed in Figure 2-2, Δz_L, the maximum liquid terminus travel is less than the distance between CHF and OFB positions. For the computation, $\Delta z_L/D_H$ will be assumed to be 1.0. Computation of $h_W(\Delta z_L)$ yields a value of 663 Btu/h-ft^2 - °F, 40 percent of the measured value. The agreement is poor, indicating that the behavior may not be sufficiently slow for the quasi-static assumption to be valid or that other factors not yet examined may influence the behavior. Improved knowledge of coefficient space dependence and terminus travel will be sufficient to predict transition boiling heat transfer.

SECTION VI

CONCLUSIONS

A model for fully-developed film boiling has been developed. It consists of heat transfer from a dry, heated surface to a slightly bulk-superheated steam phase. This heat transfer can be computed by means of modified Sieder-Tate Equations (4) or (5). The amount of steam phase superheat is governed by a coefficient for heat absorption by droplets carried with the steam. Values of absorption coefficients were computed for a number of experimental data. A mean of these values gives a good estimate of the superheat, and permits computation of an over-all film boiling coefficient.

Space-dependent film boiling coefficients may be computed by combining the thermal boundary layer development effect, given by approximate relation 16, with the bulk superheat accumulation effect, given exactly by Equation (23), by means of the combining Equation (25).

Transition boiling temperature fluctuations are related to liquid film travel and space-dependent film boiling coefficients.

NOMENCLATURE

A_H	Heated area
C_p	Specific heat
D	Diameter
D_H	Local hydraulic diameter
d	Rod diameter
f	Friction factor
G	Mass velocity
H	Heat transfer coefficient from steam to liquid
h	Heat transfer coefficient or enthalpy
j	Temperature ratio
k	Thermal conductivity or enthalpy ratio
L	Boiling heated length
p	Pressure
Pr	PRANDTL number
R	Hydraulic radius
Re	Reynolds number
S	Temperature ratio
T	Temperature
ΔT	Temperature above saturation

NOMENCLATURE (Continued)

t	Time
U	Velocity
V_T	Total volume
W	Mass rate
X	Steam quality
y	Radial coordinate
z	Axial dry wall coordinate
Δz_L	Liquid film travel
α	Void fraction
δ_T	Thermal boundary layer thickness
μ	Viscosity
ν	Kinematic viscosity
ρ	Density
ϕ	Heat flux
ϕ_c	Critical heat flux

Subscripts

A	Actual
B	Bulk steam phase
B. L.	Boundary layer
E	Equilibrium

NOMENCLATURE (Continued)

Subscripts

f	Saturated liquid
g	Saturated steam
L	Liquid
o	Over-all
S	Saturated
SUP.	Superheat
U.B.	Upper bound
W	Wall

REFERENCES

1. Quinn, E. P., "Single Rod, Forced Flow, Transition Boiling Heat Transfer from Smooth and Finned Surfaces," GEAP-4786 (1965).

2. Kunsemiller, D. F., "Multirod, Forced Flow, Transition and Film Boiling Measurements," GEAP-5073 (1965).

3. Quinn, E. P., and Swan, C. L., "Visual Observations of Fluid Behavior in High-Pressure Transition Boiling Flows," GEAP-4636/EURAEC 1258 (1964).

4. Gaudiosi, G., "Experimental Results on the Dependence of Transition Boiling Heat Transfer on Loop Flow Disturbances," GEAP-4785 (1965).

5. Sorlie, T., Task A-3, "Twelfth Quarterly Progress Report, Transition Boiling Heat Transfer Program," GEAP-5081 (October - December 1965).

6. Polomik, E. E., Levy, S., Sawochka, S. G., "Heat Transfer Coefficients with Annular Flow During 'Once-Through' Boiling of Water to 100 Percent Quality at 800, 1100, and 1400 psi," GEAP-3703 (1961).

7. Bennet, A. W., Kearsey, H. A., Keeys, R. K. F., "Heat Transfer to Mixtures of High Pressure Steam and Water in an Annulus," AERE-R4352 (1964).

8. Bennet, A. W., Kearsey, H. A., "Heat Transfer to Steam-Water Mixtures Flowing in Tubes in the Post Burnout Condition," AERE-M1449 (1964).

9. Hench, J. E., "Transition and Film Boiling Data at 600, 1000, and 1400 psia in Forced Convection Heat Transfer to Water," GEAP-4492/EURAEC 1983 (1964).

10. Parker, J D., Grosh, R. J., "Wall Temperature Variation for Mist Flowing Through Tubes with Constant Heat Flux," ASME Paper No. 62-HT-47 (1962).

11. Polomik, E. E., "Vapor Voids in Flow Systems from a Total Energy Balance," GEAP-3214 (1959).

12. Sutherland, W. A., and Miller, C. W., "Heat Transfer to Superheated Steam - Improved Performance with Turbulence Promoters," GEAP-4749 (1964).

REFERENCES (Continued)

13. Laverty, W. F., Rohsenow, W. M., "Film Boiling of Saturated Liquid Flowing in a Vertical Tube (Nitrogen)," ASME Paper No. 65-WA/HT-26 (1965).

14. Hartnett, J. P., "Experimental Determination of the Thermal-Entrance Length for the Flow of Water and of Oil in Circular Pipes," Transactions of the ASME (1955).

15. Deissler, R. G., "Turbulent Heat Transfer and Friction in the Entrance Regions of Smooth Passages," Transactions of the ASME (1955).

APPROVED: E. P. Quinn

E. P. Quinn, Project Engineer
Transition Boiling Heat Transfer Program

D. H. Imhoff

D. H. Imhoff, Manager
Engineering Development

DISTRIBUTION LIST

	No. Copies
USAEC San Francisco Operations Office 2111 Bancroft Way Berkeley 4, California 94704	
Attn: Director, Reactor Division	22
Attn: Director, Contracts Division	2
USAEC Division of Reactor Development Washington 25, D. C. 20545	
Attn: R. M. Scroggins	2
Chief, Fuels and Materials Development Branch	1
Office of Civilian Power, Water Reactors Branch	1
Assistant Director for Naval Reactors	1
Office of Army Reactors, Technical Evaluation Branch	1
Office of Nuclear Safety, Research & Development Branch	1
Assistant Director, Office of Foreign Activities	1
USAEC Division of Safety Standards Washington, D. C. 20545	
Attn: R. Impara	1
Aeroject-General Nucleonics P. O. Box 77 San Ramon, California	
Attn: K. Johnson	1
Allis-Chalmers Manufacturing Co. Atomic Energy Division Milwaukee 1, Wisconsin	
Attn: K. F. Neusen	1
Argonne National Laboratory Reactor Engineering Division 9700 South Cass Avenue Argonne, Illinois	
Attn: Dr. Paul Lottes	1
Argonne National Laboratory Reactor Engineering Division 9700 South Cass Avenue Argonne, Illinois	
Attn: Dr. M. Petrick	1
Atlantic Research Nuclear Corp. Shirley Highway at Edsall Road Alexandria, Virginia	
Attn: Dr. M. Markels, Jr.	1

DISTRIBUTION (Continued) — No. Copies

Atomics International
P. O. Box 309
Canoga Park, California
Attn: Dr. L. Bernath — 1

Babcock & Wilcox Company
Atomic Energy Division
1201 Kemper Street
Lynchburg, Virginia
Attn: D. F. Judd — 1

Brookhaven National Laboratory
Chemical Engineering Division
Upton, L. I., New York
Attn: Dr. O. E. Dwyer — 1

Dartmouth College
Thayer School of Engineering
Hanover, New Hampshire
Attn: Dr. G. B. Wallis — 1

Dynatech Corporation
17 Tudor Street
Cambridge, Massachusetts
Attn: Dr. A. Bergles — 1

General Electric Company
Advanced Technology Laboratory
Schenectady, New York
Attn: Dr. Novak Zuber — 2

Battelle Memorial Institute
Pacific Northwest Laboratory
P. O. Box 999
Richland, Washington
Attn: Dr. John Batch — 1

Geoscience Ltd.
8686 Dunaway Drive
La Jolla, California
Attn: Dr. H. F. Poppendiek — 1

Massachusetts Institute of Technology
Department of Mechanical Engineering
Cambridge 39, Massachusetts
Attn: Dr. W. M. Rohsenow — 1

Massachusetts Institute of Technology
Department of Mechanical Engineering
Cambridge 39, Massachusetts
Attn: Dr. P. Griffith — 1

North Carolina State University
Department of Chemical Engineering
Raleigh, North Carolina
Attn: Dr. J. K. Ferrell — 1

Oak Ridge National Laboratory
P. O. Box Y
Oak Ridge, Tennessee
Attn: Dr. H. W. Hoffman — 1

DISTRIBUTION (Continued)

	No. Copies
University of Minnesota Department of Chemical Engineering Minneapolis, Minnesota 55455 Attn: Dr. H. S. Isbin	1
Westinghouse Electric Corporation Bettis Atomic Power Laboratory P. O. Box 79 West Mifflin, Pennsylvania 15122 Attn: Dr. L. S. Tong	1
National Aeronautics & Space Administration Lewis Research Center 21000 Brookpark Road Cleveland 35, Ohio Attn: R. Weltmann (SEPO)	2
National Aeronautics & Space Administration Lewis Research Center 21000 Brookpark Road Cleveland 35, Ohio Attn: Library	3
Centre d'Etudes Nucléaires Chemin des Martyrs Grenoble (Isère) France Attn: M. Mondin	1
CISE Casella Postale 3986 Milano (Segrate) Italy Attn: Prof. M. Silvestri	1
MAN Abholfach Nurnberg 2 Germany Attn: Dr. Mayinger	1
SNECMA Division Atomique 22 quai Gallieni Suresnes (Seine) France Attn: M. Foure	1
Technische Hogeschool P. O. Box 313 Eindhoven Netherlands Attn: Prof. Dr. M. Bogaardt	1
Ansaldo Dirazione Generale Piazza Carignano 2 Genova Italy Attn: Dr. F. Cristofori	1

DISTRIBUTION (Continued)	No. Copies
Compagnie Francaise Thomson-Houston 1 rue des Mathurins Bagneux (Seine) France Attn: M. LeFranc	1
AEG AEG Hochhaus 6 Frankfurt (Main) S 10 Germany Attn: M. Schuller	1
Alsthom 38 Avenue Kleber Paris 16e France Attn: M. P. Domenjoud	1
Centre d'Etudes Nucléaires de Saclay B. P. n° 2 Gif sur Yvette (Seine & Oise) France Attn: M. J. Horowitz	1
FIAT Sezione Energia Nucleare Via Settembrini 235 Torino Italy Attn: M. G. Cesoni	1
Reactor Centrum Nederland 112 Scheveningseweg 's Gravenhage Netherlands Attn: Prof. Dr. M. Bogaardt	1
Euratom Director Generale R & E 51 Rue Belliard Bruxelles Belgium Attn: Dr. P. Kruys	2
Euratom Casella Postalle n° Ispra (Varese) Italy Attn: M. R. Morin	1
Division of Technical Information Extension U. S. Atomic Energy Commission P. O. Box 62 Oak Ridge, Tennessee	3 plus negatives